

Adsorption of bisphenol A and 2,4,5-trichlorophenol onto organo-acid-activated bentonite from aqueous solutions in single and binary systems

Nassima Djebri^{a,b}, Mokhtar Boutahala^{b,*}, Nacer-Eddine Chelali^a, Nadia Boukhalifa^b, Zerroual Larbi^b

^aLaboratoire Matériaux et systèmes Electroniques (LMSE), Faculté des Sciences et de la Technologie, Université de Bordj Bou Arreridj, El Annasser, 34000 BBA, Algeria, email: nessmadjebri@yahoo.fr (N. Djebri), chelalin58@yahoo.fr (N. Chelali)

^bLaboratoire de Génie des Procédés Chimiques (LGPC), Faculté de Technologie, Université Ferhat Abbas Sétif-1, 19000 Sétif, Algeria, , email: mboutahala@yahoo.fr (M. Boutahala), nadouchette2011@hotmail.fr (N. Boukhalifa), zerroual@yahoo.fr (Z. Larbi)

Received 10 March 2016; Accepted 9 September 2016

ABSTRACT

The organo-acid-activated bentonite (OAB) was prepared and characterized by SEM, XRD, FTIR, pH_{PZC} and BET. Then the OAB was employed as adsorbent for the removal of bisphenol A (BPA) and 2,4,5-trichlorophenol (TCP) from aqueous solutions. The adsorption performances of OAB were investigated by batch mode experiments with respect to pH, temperature, initial concentration, contact time and competitive adsorption. The Langmuir model describes better the results of BPA adsorption while the results of TCP are best fitted to Freundlich model. The maximum adsorption capacities are found to be 127.7 and 244.6 mg/g for BPA and TCP, respectively. The kinetic properties were well described by the pseudo-second-order equation. Thermodynamic parameters suggest that the adsorption process of BPA and TCP onto organoclay (OAB) are physisorption, spontaneous and exothermic. In binary solutions, BPA and TCP show competitive adsorption. Hydrophobic interaction play an important role during the sorption process. In addition, OAB could be regenerated and reused for adsorption of BPA/TCP again.

Keywords: Endocrine-disrupting compounds; Removal; Bisphenol A; 2,4,5-TCP; Organo-clay

1. Introduction

Endocrine disrupting chemicals (EDCs), which derive from various kinds of chemicals including drugs, pesticides, consumer products, industrial by-products and pollutants and even some naturally produced botanical chemicals, have been known to have a potential threat to the health of mankind and ecological environment [1,2]. In this context, the phenolic compounds such as bisphenols (bisphenol-A, BPA), chlorophenol (CP), octylphenol (OP), nonylphenol (NP) are considered among the EDCs because of their high toxicity, whereas, BPA was found to be the main EDCs which has been used as a coating chemical on a metal surface in order to increase the resistance against corrosion [3]. On the other hand, Chlorophenol and their derivatives

(such as trichlorophenol) belong to the EDCs, 2,4,5-trichlorophenol (TCP) it is the main toxic compound because of its phenolic ring structure, with three chlorine atoms [4]. It is commonly found in industrial wastewaters activities and identified as persistent bioaccumulation and toxic pollutant [3,5]. Related to the above, these phenolic compounds (BPA and TCP) are classified as pollutants [3,4] that are known to be toxic, carcinogenic, and thereby pose serious hazards to aquatic living organisms. Indeed, it is necessary to remove these pollutants from wastewaters before discharge into the environment [6,7].

Nowadays, several techniques including oxidation processes [8,9], photocatalytic degradation [10], biodegradation [11], adsorption [12–14] have been utilized for the treatment of BPA and TCP from aqueous systems. Among these methods, adsorption is the most effective and convenient method because of its comparatively low cost,

*Corresponding author.

ease of operation and production of less secondary products [15,16]. Previously, several adsorbents were used for the removal of BPA and TCP from aqueous medium, surfactant-modified zeolite [7,17], activated carbon [3,12], polymer-based materials [4,5,18,19] and cationic-modified clay [20,21].

Natural bentonites are argillaceous materials that have been widely used to remove toxic metal ions, dyes, chlorophenols and drugs [16]. Due to their high specific surface area, high cation exchange capacity (CEC) and chemical and physical stability, they can be effectively employed as adsorbents for many wastewater pollutants. To improve adsorption of organic pollutants, many researchers have focused on the surface modifications by exchanging interlayer inorganic cations (e.g., Na^+ , K^+ , Ca^{2+}) with organic cations such as quaternary alkylammonium. The modification of the bentonite with surfactant molecules changes the properties of the bentonite from hydrophilic to hydrophobic and organophilic. It also increases the basal spacing of the layers. Thus, organophilic bentonite can have various applications, especially as adsorbents for a great variety of organic pollutants [11,16].

Another modification of bentonite is the treatment of clay minerals with concentrated inorganic acids usually at high temperature. This process is known as acid activation. Acid activation consists of the reaction of clay minerals with a mineral acid solution, usually HCl or H_2SO_4 . The goal of this activation is to obtain a partly dissolved material with increased surface specific area, porosity, surface acidity and improve the adsorption properties of the clay by increasing the number of active sites [22].

Depending on the materials used and the modification procedure, the cost of adsorbent is different. In previous works, adsorption of the TCP was studied onto Algerian bentonite converted to Na-montmorillonite, activated with sulfuric acid [20], onto Na-montmorillonite exchanged with hexadecyltrimethylammonium (MtC16) [16] and acid-organomontmorillonite (AMt-C16) [20]. In contrary to the previous works, the modification procedure used in this study is simple. The mineral was not converted into homoionic form; this factor decreases the cost of the production of adsorbents. Natural bentonite was activated with sulfuric acid and exchanged with hexadecyltrimethylammonium bromide at 100% CEC.

In the present study, raw bentonite (RB), acid-activated bentonite (AB) and organo-acid-activated bentonite (OAB) were analyzed and characterized by SEM, BET, XRD, FT-IR and pH_{PZC} . BPA and TCP were selected as model phenolic pollutants to examine the performance of OAB in single and binary solutions by batch mode experiments. Finally, to implement an easy regeneration technique and application to recover adsorbent (OAB) from the solution after adsorption. However, the published information on the adsorption of BPA/TCP in single and binary systems, and also regeneration study for the organo-acid-activated bentonite is limited in our knowledge.

2. Materials and methods

2.1. Materials

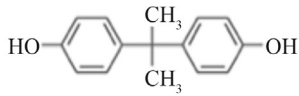
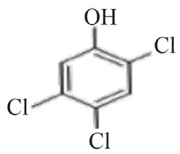
The bentonite (RB) used in this study was obtained from Hammam Boughrara in Maghnia (West Algeria). The chemical composition of the original clay was reported in our earlier publication [23]. The surfactant used for the preparation of organoclay is CTAB ($\text{C}_{19}\text{H}_{42}\text{NBr}$, >98%), which is obtained from Sigma-Aldrich. Bisphenol A (BPA), 2,4,5-trichlorophenol (TCP), sodium chloride, sulfuric acid were also purchased from Sigma-Aldrich. The physicochemical properties of phenolic compounds are given in Table 1. All other chemicals and solvents used in this research were analytical grade. Distilled water was used in all experiments.

2.2. Preparation of organo-acid-activated bentonite (OAB)

The purified bentonite was subjected to acid treatment with sulfuric acid. Acid leaching was carried out by placing the sample in contact with H_2SO_4 1M (1:1 w/w) with stirring and reflux heating (90°C) for 5 h. The resulting solid was immediately centrifuged, washed with distilled water until it was free from sulfate ions, dried at 80°C and named: AB.

In order to increase its hydrophobicity by co-adsorption with a surfactant, a suspension of AB was treated with cetyltrimethylammonium bromide (CTAB) by adding the amount of the cationic surfactant equivalent to 100% of the value of CEC. The surfactant was dissolved in 1 L of distilled water at 80°C and stirred for 3 h. 10 g of sample (AB) were added to the surfactant solution. The dispersion was

Table 1
Physicochemical properties of the selected phenolic EDCs

Compound	MW ($\text{g} \cdot \text{mol}^{-1}$)	Water solubility ($\text{mg} \cdot \text{L}^{-1}$), at 25°C	Dissociation constant (pKa)	$\log K_{ow}$	Chemical structure
Bisphenol A ($\text{C}_{15}\text{H}_{16}\text{O}_2$)	228.29	120–300	9.6–10.2	3.32	
TCP ($\text{C}_6\text{H}_3\text{Cl}_3\text{O}$)	197.45	1200	6.7–6.94	3.66	

stirred for 3 h at 80°C. The resulting solid, named OAB, was separated, washed several times with distilled water until the supernatant solution was free of bromide ions and dried at 80°C for 48 h.

2.3. Characterization of adsorbents (RB, AB and OAB)

The morphological structure of the investigated samples was examined by scanning electron microscopy (SEM) using JSM-6830LV, JEOL SEM model.

Fourier transform infrared spectra (FT-IR) before and after modification were recorded on a Mattson 5000 FTIR spectrometer in the range between 400 and 4000 cm⁻¹.

Specific surface area (S_{BET} , m²/g), total pore volume (V_T , cm³/g), and micropore volume (V_{μ} , cm³/g) were determined via nitrogen adsorption at 77 K (out-gassing was carried out at 100°C) using a NOVA2000 gas adsorption analyzer (Quantachrome Corporation, USA) system.

X-ray diffractograms were obtained using a Bruker D8 advance Diffractometer operating at 40 kV and 30 mA with Cu K_α radiation ($k = 0.15406$ nm). Radial scans were recorded in the reflection scanning mode from $2\theta = 2-80^\circ$. Bragg's law, defined as $n\lambda = 2d \sin 2\theta$, was used to compute the Crystallographic (d) for the examined clay samples.

The pH_{PZC} (point of zero charge) values of RB, AB and OAB (Figure not shown) were obtained using published method [16]. The experimental determination of pH_{PZC} of samples RB, AB and OAB have been determined respectively as 7.20, 4.92 and 5.90. At these points, surfaces of the adsorbents had zero net charge

2.4. Single adsorption studies

The adsorption of BPA and TCP was conducted in batch experiment. Aqueous solutions of certain concentrations of adsorbate were shaken in flask bottles of 50 mL capacity with 50 mg of adsorbent (OAB) under agitation for 4 h. The supernatant liquid was centrifuged out and the equilibrium concentration of BPA and TCP were determined using UV-Vis spectra (Shimadzu UV-1700 UV/VIS spectrophotometer) at 276 nm and 290 nm, respectively.

The effect of various parameters: initial BPA and TCP concentration, adsorbent dose, pH, temperature and contact time on BPA and TCP uptakes were investigated. The BPA and TCP removal percent ($R\%$) and uptake the capacity (q_e) (mg · g⁻¹) were estimated respectively using the following equations:

$$R(\%) = \frac{(C_0 - C_e) \cdot 100}{C_0} \quad (1)$$

$$q_e = \frac{(C_0 - C_e) \cdot V}{m} \quad (2)$$

where C_0 and C_e are the initial and equilibrium concentration (mg · L⁻¹) of adsorbate solution, respectively; V is the volume of working solution (L) and m is the weight (g) of adsorbent used.

2.5. Binary adsorption studies

The first step was to examine the adsorption of BPA at equilibrium (concentration of BPA ranging from 20 to 700 mg · L⁻¹) in the presence of TCP (100 mg · L⁻¹). For the next step, a series of binary solutions where the concentration of BPA was fixed at 100 mg · L⁻¹, and concentration of TCP was varied from 20 to 800 mg · L⁻¹. These binary solutions were also agitated at 200 rpm for 4 h. In this experiment, the adsorption temperature was fixed at $25 \pm 1^\circ\text{C}$, and the solution pH was 7.0 for the first step and 4.0 for the second step, respectively. A correction was applied for the spectrophotometric determination of residual concentrations in mixture systems by using the Eq. (4):

$$C_{BPA} = \frac{k_{TCP2}d_{\lambda 1} - k_{TCP1}d_{\lambda 2}}{k_{BPA1}k_{TCP2} - k_{BPA2}k_{TCP1}} \quad (3)$$

$$C_{TCP} = \frac{k_{BPA1}d_{\lambda 2} - k_{BPA2}d_{\lambda 1}}{k_{BPA1}k_{TCP2} - k_{BPA2}k_{TCP1}} \quad (4)$$

where C_{BPA} , C_{TCP} , k_{TCP1} , k_{TCP2} , k_{BPA1} , k_{BPA2} , $d_{\lambda 1}$ and $d_{\lambda 2}$ are respectively the concentration of BPA and TCP, the calibration constants for the BPA and TCP at their characteristic adsorption wavelength (i.e., k_1 and k_2), and the optical densities at the two wavelengths k_1 and k_2 .

2.6. Desorption of BPA/TCP and reuse of OAB studies

Desorption study was conducted using ethanol as desorption eluent for 2 h at $25 \pm 1^\circ\text{C}$. Adsorption was first conducted using the optimal procedure in Section 2.4. The initial concentration of adsorption was 100 mg · L⁻¹ for BPA and TCP. Then the OAB with adsorbed TCP or BPA were separated rapidly from the solutions. Subsequently, the supernatant solutions were discarded and the OABs were washed several times with distilled water. Finally, the TCP (or BPA) was desorbed from the OAB with ethanol solution. The regenerated material was washed several times with distilled water, dried in an oven and used for the next adsorption desorption studies and the process was repeated for four times. The percentage of desorption was calculated as:

$$R\% = \frac{m_{des}}{m_{ads}} \times 100 \quad (5)$$

where m_{des} (mg) and m_{ads} (mg) are the amounts of desorbed and adsorbed BPA or TCP, respectively.

2.7. Analysis of the data

Each data point was taken as the average of three measurements with a standard deviation of 2%. When the relative error exceeded 2.0%, the data were discarded and a new experiment was conducted until the relative error falls within an acceptable range. The values of the kinetic and isotherm parameters (in single and binary studies) were determined by a nonlinear regression analysis using ORIGIN program (version 8.5). The nonlinear R^2 (correlation coefficients) were used to analyse the data set to confirm the

best fit kinetics and isotherm model for the adsorption. If data from the model are similar to those obtained in experiments, R^2 will be close to one.

3. Results and discussion

3.1. Characterization of RB, AB, and OAB

SEM images of the samples are presented in Fig. 1. Fig. 1a and b indicate SEM images of acid activated bentonite. The image shows irregular shape of the particles with more compact arrangement with netting. Some small needed pores in the image may indicate high surface area and hence it may acts as good adsorbent properties [24]. How-

ever, the AB treated with organic surfactant shows significant changes in the morphology (Fig. 1c, d). Compared with the morphology of the bentonite, there are many small and aggregated particles and the plates become relatively flat layers. Due to an increase of basal spacing in organoclays more voids are seen [25].

The XRD results of RB, AB and OAB are presented in Fig. 2. The peak for the d -spacing of RB is observable at $2\theta = 6.8^\circ$. According to Bragg's equation, the d -spacing (001 reflection) of RB is 13.4 Å. An increase of 001 reflection is noticed as the acid activation occurred. However, the intensity of the 110 reflection (at 4.47 Å) varied slightly, due to the less variation of the chemical composition of the RB layers during acid activation. Activation has also affected the 060 reflection (partial dissolution of Fe^{3+}). The intensity of the

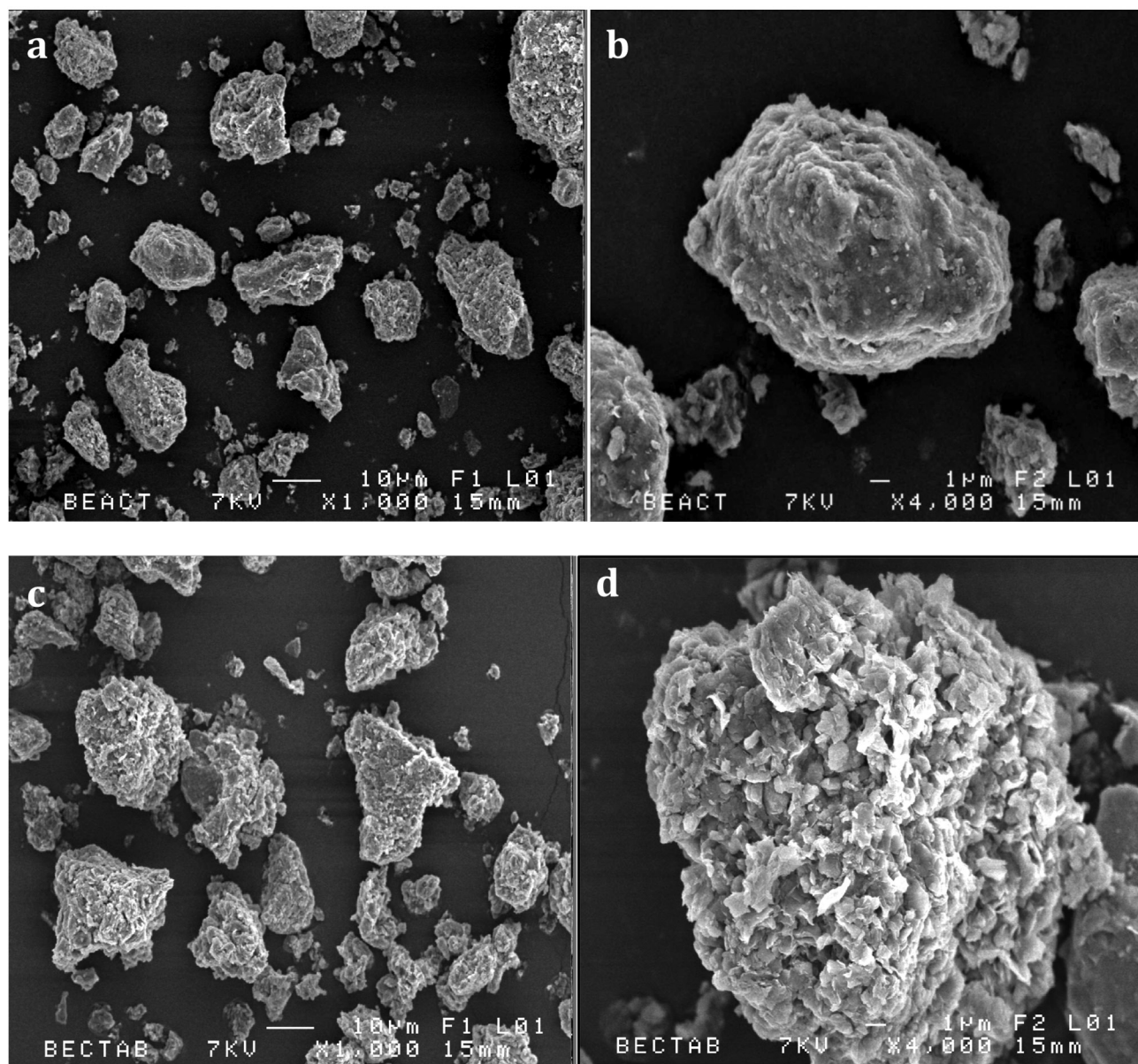


Fig. 1. SEM images of AB (a, b) and OAB (c, d).

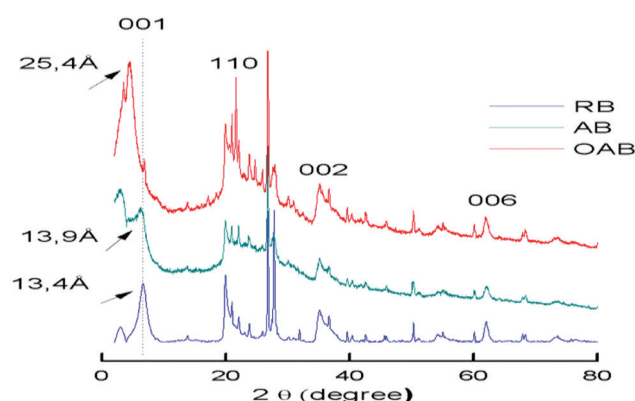


Fig. 2. XRD patterns of RB, AB and OAB.

d_{060} reflection has been reduced [23,26]. Additional phases resulted from the acid treatment were observed due to some impurities in the starting clay mineral. Activated bentonite (AB) has a basal spacing of 13.9 Å, which increased when H^+ ions were replaced with quaternary ammonium cations. At 1.0 CEC surfactant concentration, the basal spacing is 25.4 Å for OAB. This value indicated a lateral bilayer or pseudo trimolecular layer arrangement with the surfactant molecules within the clay layers either flat or perpendicular to the clay siloxane surface [22]. When organic cations replaced H^+ ions, surfactant CTAB mainly adhered to surface sites via electrostatic interactions. Similar data were obtained by Gomri et al. [26].

In order to obtain complementary evidence for the intercalation of quaternary alkylammonium cations into the silicate lattice, the materials were characterized by FT-IR analytical methods and results clearly demonstrated that a pair of strong bands (Fig. 3) 2853 and 2921 cm^{-1} , were observed only on organo-acid-bentonite (OAB); they can be assigned to the symmetric and antisymmetric stretching vibrations of methylene group (νCH_2). Other bands appeared on the spectra of the organo-acid-activated bentonite at 1475 and at 722 cm^{-1} . These two bands are attributed to the scissoring and rocking vibration of the methylene group (CH_2), respectively. The band at 1639 cm^{-1} is attributed to water bending modes within the clay interlayer [16,20]. The intensity of this band decreases with intercalation of surfactant molecules between the silica layers. The 3420 cm^{-1} band intensity decreases also

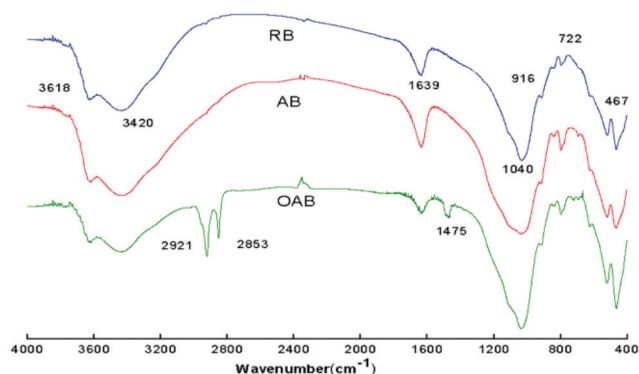


Fig. 3. FT-IR spectra of RB, AB and OAB.

when compared with the original bentonite showing that water of hydration is lost as the cation (H^+) is replaced by the cationic surfactant. This enabled that the cationic molecule was introduced within the clay network for the OAB.

The nitrogen adsorption-desorption isotherms at 77 K for RB, AB, and OAB samples are shown in Fig. 4, from which it can be seen that these isotherms are of type II of the Brunauer, Deming, Deming and Teller (BDDT) classification [27]. The textural properties are summarized in Table 2. The RB exhibited an S_{BET} of 84 m^2/g close to that reported for similar types of clay minerals [26]. The acid-activation has markedly affected the nitrogen adsorption characteristics of the bentonite. After the activation, the nitrogen uptake relatively increased. After exchange with surfactant solutions, the nitrogen adsorption capacity of the organo-acid-activated-bentonite decreases. The results included in Table 2 show also that specific surface area and pore volume of AB decreased from 337 m^2/g and 0.335 cm^3/g to 180 m^2/g and 0.285 cm^3/g for OAB. This indicates that surfactant with large molecular size occupied part of the interlayer space resulting in inaccessibility of the internal surface to nitrogen molecules and blocked the pores of the OAB organobentonite material [28–30]. The micropore volume compared with a mesopore volume (see Table 2) of the samples indicates that bentonite has high mesoporosity. From these results, it was assumed that the surface area and pore volume are not important factors in terms of controlling the affinity between organoclay and organic pollutants. Hence the loaded surfactant is highly important for determining the adsorption mechanism onto organoclays [20].

3.2. Effect of pH solution on BPA and TCP adsorption

The effect of pH on the removal of BPA and TCP by OAB is shown in Fig. 5. From the data, it was observed that maximum removal was found to be at a pH 4 and 7 for TCP and BPA, respectively, thereafter it decreases. As can be seen, the removal was found to be highly dependent on the hydrogen ion concentration of the solution. The maximum removal was found to be 89.0 and 92.5 $mg \cdot g^{-1}$ for BPA and TCP, respectively. Thus, the pH of 4.0 and 7.0 were chosen as an optimum pH for all subsequent experiments. Bisphenol and chlorophenol are weakly acidic, and the pH has

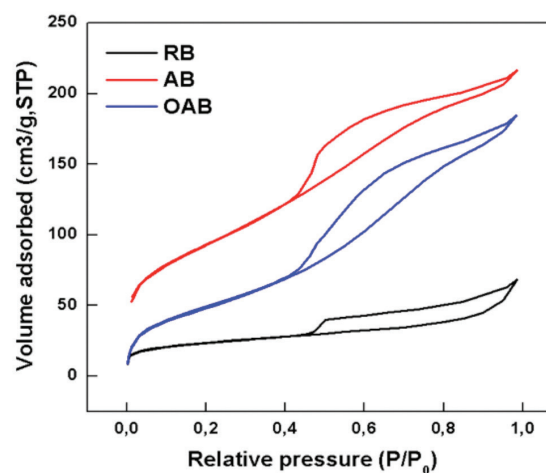


Fig. 4. N_2 adsorption-desorption isotherms for RB, AB and OAB.

Table 2
Textural parameters of samples

Samples	S_{BET} ($\text{m}^2 \cdot \text{g}^{-1}$)	S_{ext} ($\text{m}^2 \cdot \text{g}^{-1}$)	V_{PT} ($\text{cm}^3 \cdot \text{g}^{-1}$)	V_{HP} ($\text{cm}^3 \cdot \text{g}^{-1}$)	d_{001} (Å)	pH_{PZC}
RB	84	32	0.105	0.026	13.4	7.20
AB	337	42	0.335	0.254	13.9	4.92
OAB	180	55	0.286	0.180	25.4	5.90

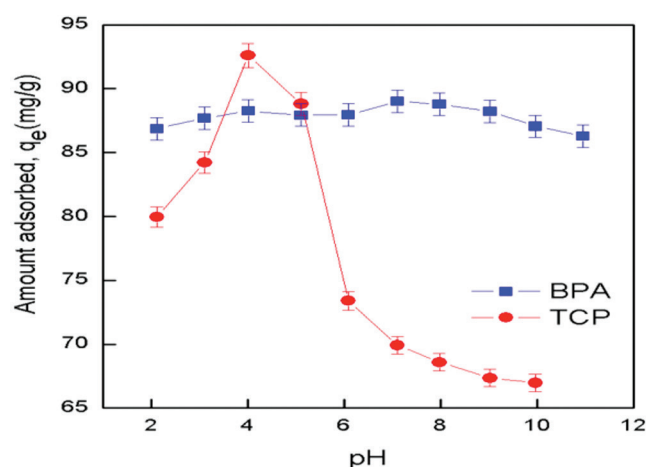
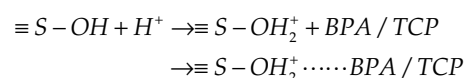


Fig. 5. Effect of pH in adsorption of BPA and TCP onto OAB ($V_{\text{sol}} = 50 \text{ mL}$; $m_{\text{ads}} = 50 \text{ mg}$; $T = 25 \pm 1^\circ\text{C}$, $C_0 = 100 \text{ mg/L}$).

a significant effect on the degree of ionization and charge of TCP and BPA. The amount of adsorbed phenols seems to be related to the dissociation constant (pKa), which is (9.6–10.2) and (6.7–6.94) for BPA and TCP, respectively. The ionic fraction of the phenols ions increased with increasing pH, and phenolate became negatively charged as the pH increased. The effect of pH can be explained by considering the surface charge and isoelectric point (pH_{PZC}) of the organoclay (OAB). The pH_{PZC} value of OAB is 5.90. The solid surface carried net positive charge below this pH. Beyond this pH value, the surface carried net negative charge with the dissociation of surface functional group. At higher pH, the repulsion of the negatively charged BPA or TCP species and the dissociation of functional groups of adsorbent may decrease the interaction of adsorption system. In addition, the competitive adsorption of OH^- ions can also result in a decrease in adsorption capacity. Accordingly, at lower pH, an electrostatic attraction occurs between the BPA/TCP molecules and the positively charged clay surface as following:



It is well known that the adsorption of organic compounds onto the modified clay is controlled by two mechanisms for the adsorption of phenols on organoclays at low pH values; electrostatic attraction because the presence of excess hydrogen ions results in a more positive charge on the clay layers, and partition interaction when the BPA/TCP

exist in the molecular form [16,20]. So, the results strongly suggested that BPA and TCP were trapped by OAB through the hydrophobic interaction and the hydrogen-bonding interaction simultaneously. These results suggest that the pH value of the phenol solution plays an important role in the whole adsorption process, particularly in the adsorption capacity.

3.3. Effect of adsorbent dose

The dependence of removal efficiency of BPA and TCP on the OAB adsorbent dosage was investigated, (figure not showed), The adsorbent mass varied from 20 to 100 mg keeping the BPA and TCP concentration constant ($50 \text{ mg} \cdot \text{L}^{-1}$), the temperature $25 \pm 1^\circ\text{C}$ and pH 4 for TCP and pH 7 for BPA. The results show that the removal percentages increase with the increasing of adsorbent dose up to 100 and 60 mg, for BPA and TCP, respectively. In addition, it was found that the increasing rates of removal efficiency became slower when the OAB dose increases, which is probably due to the greater adsorbent surface area and pore volume available, providing more functional groups and active adsorption sites that result in a higher removable percentage [18].

3.4. Effect of initial concentration

The adsorption of BPA/TCP was kinetically studied and the results are presented in Fig. 6. As shown in Fig. 6, the removal of BPA and TCP occurred in a similar way and OAB presents a slightly higher adsorption capacity of TCP than BPA. The adsorption of BPA/TCP were fairly rapid on OAB to reach equilibrium within 20 min which could be explained by the direct electrostatic attraction on the outside surface or inner space of the adsorbent [20]. Furthermore, the adsorbent with large pores also can accelerate the adsorption reaction to shorten the equilibrium time. TCP and BPA removal linearly increase with time, and a pseudo-equilibrium TCP/BPA removal state was established within 20 min for OAB. The transport of BPA/TCP from the solution to the sorbent occurred in two stages, namely, the external surface sorption or faster sorption stage, and the interior surface sorption or gradual sorption stage. Most of the BPA/TCP mass transfers to the sorbent particles occurred during the first stage, which possibly corresponds to macropore and mesopore diffusion. On the other hand, the second stage may be related to micropore diffusion. Therefore, adsorption capacities of BPA and TCP onto OAB increased from 48.8 to 89.3 $\text{mg} \cdot \text{g}^{-1}$ and from 50 to 92.6 $\text{mg} \cdot \text{g}^{-1}$ with increasing initial BPA and TCP concentration, respectively.

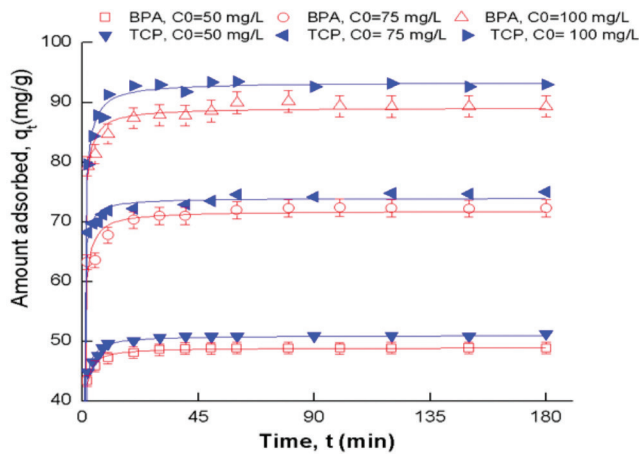


Fig. 6. Effect of contact time and initial concentration on the adsorption of BPA and TCP onto OAB (pH = 4 and 7, $m_{ads} = 50$ mg, $V_{sol} = 50$ mL, $T = 25 \pm 1^\circ\text{C}$).

3.5. Kinetic model

In order to examine the mechanism and rate-controlling step in the overall adsorption process, several models have been reported in literature. Two well-known kinetic models namely, pseudo-first-order (PFO), pseudo-second-order (PSO) kinetic models were tested to fit the experimental kinetic data. Comparing the correlation coefficient (R^2) values, we found that the adsorption kinetics was best described by the pseudo-second-order model. The specific rate constants of TCP/BPA adsorption on OAB were determined using the following pseudo-second-order rate expression [34]:

$$q_t = \frac{k_2 q_e^2 t}{1 + k_2 q_e t} \quad (6)$$

where q_e and q_t are the amounts of TCP/BPA adsorbed ($\text{mg} \cdot \text{g}^{-1}$) at equilibrium and at time t (min), respectively and k_2 ($\text{g} \cdot \text{mg}^{-1} \cdot \text{min}^{-1}$) is the rate constant of second-order kinetic model. The kinetic parameters were determined using non-linear regression analysis and the results are presented in Table 3. The adsorption kinetic of TCP/BPA onto OAB was best described by the pseudo-second-order model because the R^2 values were higher than those of the pseudo

first order model at in all initial concentrations. This supports the assumption that the rate determining step may be chemisorption involving sharing or exchange of electrons between adsorbent and adsorbate. Fig. 6 shows an excellent fit between experimental data and calculated pseudo-second-order model. The values of q_e increased from 49.0 ($R = 98.5\%$) to 89.1 ($R = 89.9\%$) $\text{mg} \cdot \text{g}^{-1}$ and from 51.0 ($R = 100\%$) to 93.4 ($R = 93.9\%$) $\text{mg} \cdot \text{g}^{-1}$ for BPA and TCP respectively, when the initial concentration increased from 50 to 100 $\text{mg} \cdot \text{L}^{-1}$. Several authors showed the successful application of pseudo-second order model for the representation of experimental kinetics data of phenolics adsorption on organo-clay [8,28].

3.6. Adsorption mechanism

The diffusion mechanism between adsorbent and adsorbate are not elucidated well by PFO and PSO kinetic models. Weber and Morris described the intraparticle diffusion mechanism between the solutes and particles. Based on this intraparticle diffusion, it can be formulated as follows [36]:

$$q_t = k_3 t^{0.5} + C \quad (7)$$

where C is the intercept related to the boundary layer effect and k_3 ($\text{mg}/\text{g} \cdot \text{min}^{0.5}$) is the intraparticle diffusion rate constant. As shown in Table 3, the values of R^2 obtained from the linear regression plots of q_t vs $t^{0.5}$ (figure not shown) for the whole time data of the sorption process were low. The low R^2 values suggest that the Weber-Morris model could not describe well the experimental data and that the TCP/BPA adsorption process was not limited by the intraparticle diffusion.

3.7. Equilibrium isotherm studies

The equilibrium of adsorption is one of the important physico-chemical aspects in the description of adsorption behavior. Two famous isotherm equations, namely the Langmuir and Freundlich [19], were applied to fit the experimental isotherm data of BPA and TCP adsorption on OAB (Figs. 7 and 8). The non linear form of these equations can be written as:

$$\text{Langmuir isotherm: } q_e = \frac{q_m K_L C_e}{1 + K_L C_e} \quad (8)$$

Table 3
Adsorption kinetic parameters of TCP/BPA on OAB

	C_0	$q_{e,exp}$	Pseudo-first-order model			Pseudo-second-order model			Intra-particle diffusion model		
			$q_{e,cal}$	k_1	R^2	$q_{e,cal}$	$k_2 \cdot 10^{+2}$	R^2	C	$k_3 \cdot 10^{+2}$	R^2
TCP	50	49.8	50.0	1.1	0.990	51.0	6.3	0.999	45.7	32.1	0.503
	75	74.9	72.8	1.3	0.992	74.0	6.4	0.998	65.0	69.7	0.658
	100	94.0	91.5	1.0	0.989	93.4	2.9	0.998	82.0	72.6	0.627
BPA	50	49.0	48.4	1.1	0.995	49.0	7.4	0.999	47.0	42.8	0.556
	75	72.4	70.7	1.0	0.983	71.8	4.0	0.995	69.2	54.1	0.825
	100	89.0	88.0	1.1	0.989	89.1	3.8	0.997	85.3	85.4	0.457

C_0 ($\text{mg} \cdot \text{L}^{-1}$), q_e ($\text{mg} \cdot \text{g}^{-1}$), k_1 (min^{-1}), k_2 ($\text{g} (\text{mg} \cdot \text{min})^{-1}$), k_3 ($\text{mg} \cdot \text{g}^{-1} \cdot \text{min}^{-0.5}$), C ($\text{mg} \cdot \text{g}^{-1}$).

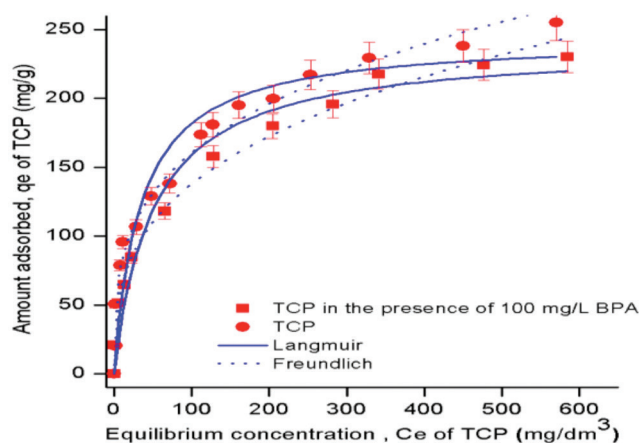


Fig. 7. Equilibrium isotherms for adsorption of TCP and (TCP in presence of 100 mg/L BPA) onto OAB.

$$\text{Freundlich isotherm: } q_e = K_f C_e^{\frac{1}{n}} \quad (9)$$

where q_m ($\text{mg} \cdot \text{g}^{-1}$) is the Langmuir maximum uptake of BPA or TCP per unit mass of OAB, K_L ($\text{L} \cdot \text{mg}^{-1}$) is the Langmuir constant related to rate of adsorption, K_F [$(\text{mg} \cdot \text{g}^{-1}) (\text{L}/\text{mg})^{1/n}$] and n are Freundlich constants which give a measure of the adsorption capacity and the adsorption intensity, respectively.

The calculated constants of the two isotherm equations along with R^2 values for both components are presented in Table 4. The applicability of the isotherm models for the adsorption behavior was studied by judging the correlation coefficient (R^2). This table shows that the Langmuir isotherm correlates experimental data with highest R^2 value for BPA, while the Freundlich isotherm correlates better the experimental for TCP, indicating that the removal of TCP on heterogeneous surfaces may involve multilayer adsorption, which also supports the proposed physisorption mechanism, similar results were obtained using halloysite clay mineral [37]. The shape of the isotherm provides information about the adsorption mechanisms. According to Giles classification of adsorption isotherm [38], the TCP/BPA adsorption onto OAB forms an L-shape curve (Figs. 7 and 8), which indicates that TCP/BPA molecules are probably adsorbed in a flat position because of low competition from solvent molecules. The Langmuir

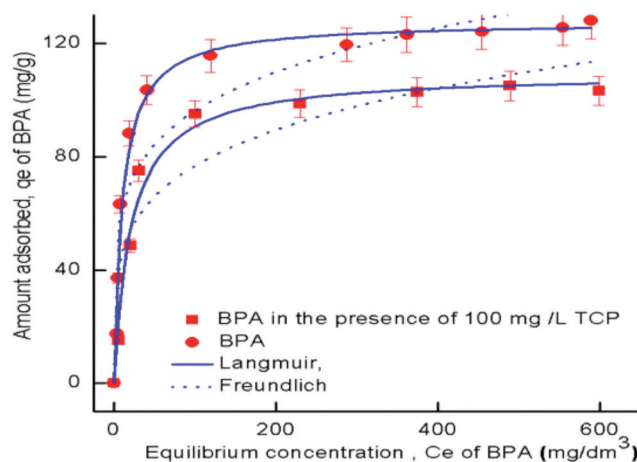


Fig. 8. Equilibrium isotherms for adsorption of BPA and (BPA in presence of 100 mg/L TCP) onto OAB.

isotherm gave maximum adsorption capacities of 127.7 and 244.6 $\text{mg} \cdot \text{g}^{-1}$ for BPA and TCP, respectively. It can be seen from this result that the uptake of TCP is higher than that of BPA; this may be due to the smaller molecular size of TCP as compared with that of BPA. It was also observed that the values of $1/n$ were all less than 1.0, indicating that the BPA and TCP adsorption onto the OAB was favorable [34,39]. So, surfactant is adsorbed on the exterior surface and are intercalated into the interlayer of clay particles. This configuration will create an effective organic environment and enhance the hydrophobicity of the organoclay (OAB), resulting in good affinity for organic molecules [35]. Table 5 lists a comparison of maximum adsorption capacities of BPA and TCP on OAB with those on different synthesized and natural materials. It can be seen that OAB can be classified as one of the effective adsorbents for this purpose. This is because the removal mechanism of chlorophenols by organoclays involves a combination of partitioning, electrostatic attraction, and van der Waals forces [35].

3.8. Thermodynamics of adsorption

The study of the temperature of adsorption of BPA and TCP onto OAB is carried out at four different values, i.e., 298, 308, 318 and 328 K. The following relationships have

Table 4

Langmuir and Freundlich parameters for adsorption TCP/BPA onto OAB in Single and binary solution systems

	TCP	TCP in presence of BPA (100 mg · L ⁻¹)	BPA	BPA in presence of TCP (100 mg · L ⁻¹)
Langmuir				
q_{max} (mg/g)	244.1	238.7	127.7	109.6
$K_L \cdot 10^{+2}$ (L · mg ⁻¹)	2.91	1.99	9.63	4.80
R^2	0.934	0.966	0.983	0.981
Freundlich				
K_F ((mg · g ⁻¹) (L/mg) ^{1/n})	42.23	31.1	39.8	27.8
$1/n$	0.289	0.323	0.191	0.22
R^2	0.983	0.991	0.876	0.876

Table 5
Comparison of the adsorption capacity

Sorbate	Sorbent	q_{max} (mg · g ⁻¹)	Ref
BPA	OAB	127.7	Present work
	Cationic-modified zeolite	37.85	[7]
	Mesoporous silicas	123	[15]
	Hybrid multi-walled carbon nanotubes-alginate-polysulfone	24.53	[18]
	Polygorskite-molecularly imprinted polymer	40.31	[19]
	Organo-montmorillonite	114.94	[21]
	Mesoporous carbon	296	[40]
TCP	OAB	244.1	Present work
	β-cyclodextrin mesoporous attapulgite composites	65.19	[4]
	Organophilic-bentonite	72.14	[20]
	Modified natural bentonite	160.4	[29]
	MgAl-SDBS organo-layered double hydroxides	240.5	[41]
	Magnetic molecularly imprinted Fe ₃ O ₄ carbon nanospheres	200	[42]

been used to evaluate the thermodynamic parameters Enthalpy ΔH° , Gibbs free energy ΔG° and entropy ΔS° [5]:

$$\Delta G = -RT \ln K \tag{10}$$

$$\log\left(\frac{1000 \times q_e}{C_e}\right) = \frac{\Delta S^\circ}{2.303R} - \frac{\Delta H^\circ}{2.303RT} \tag{11}$$

where q_e is the amount of BPA and TCP adsorbed per unit mass of OAB (mg · g⁻¹), C_e is the equilibrium concentration (mg · L⁻¹), R is the universal gas constant (8.314 J · K⁻¹ · mol⁻¹); T is temperature in Kelvin (K). From the plot of $\log(1000 \times q_e / C_e)$ vs. $1/T$ (figure not shown), the intercept and slope were used to determine the values of ΔH° and ΔS° , respectively. The thermodynamic adsorption parameters determined are summarized in Table 6. The equilibrium adsorption capacities of BPA (91.6–86.3 mg · g⁻¹) and TCP (93.0–81.0 mg · g⁻¹) decreased with a decrease in temperature from 298 to 328 K, which indicates that the adsorption of phenolic compounds is controlled by an exothermic reaction. The overall free energy change during the adsorption process was negative for the experimental range of temperature (see Table 6), corresponding to a spontaneous physical process of BPA

and TCP adsorption. The negative value of ΔG° indicates the feasibility of the process and suggests that the adsorption of BPA and TCP on OAB is spontaneous [43]. The small negative value of enthalpy change (–10.8 kJ · mol⁻¹ and –22.3 kJ · mol⁻¹ for BPA and TCP, respectively) indicates that the adsorption is physical in nature involving weak forces of attraction [20]. The low value of ΔH° implies that there is a loose bonding between the adsorbate molecules and the adsorbent surface [15,39]. The negative value of ΔS° (–0.071 J (K · mol⁻¹)) for TCP, suggests that the degree of freedom decreases at the solid–liquid interface during the adsorption of TCP on OAB.

3.9. Competitive adsorption in binary solution systems

It is well known that the competitive sorption characteristics is very important for the application of sorbents in wastewater treatment because organic pollutants usually coexist with one other [44]. The effect of competitive adsorption of BPA and TCP onto OAB at different initial concentrations is given in Figs. 7 and 8. According to this figures, the monolayer adsorption of BPA and TCP from single solution system is 127.7 and 244.1 mg · g⁻¹,

Table 6
Thermodynamic parameters for BPA/TCP adsorption on OAB

Phenolics EDCs	T (K)	q_e (mg · g ⁻¹)	ΔG° (kJ · mol ⁻¹)	ΔH° (kJ · mol ⁻¹)	ΔS° (J · mol ⁻¹ K ⁻¹)
BPA	298	91.6	–21.91	–10.8	37.40
	308	90.1	–22.29		
	318	88.2	–22.99		
	328	86.3	–23.04		
TCP	298	93.0	–22.245	–22.3	–0.071
	308	89.8	–22.244		
	318	86.3	–22.243		
	328	81.0	–22.242		

and from binary solution system is 109.62 and 238.68 $\text{mg} \cdot \text{g}^{-1}$, respectively. The q_e^b/q_e^s ratio represents the extent of sorption competition in a binary-solute solution system; q_e^b and q_e^s are the equilibrium sorption amount of BPA or TCP adsorbed per unit mass of the sorbent in binary and single-solute solutions, respectively. Adsorption agent q_e^b/q_e^s of both BPA (0.85 when the addition of $100 \text{ mg} \cdot \text{L}^{-1}$ of TCP) and TCP (0.97 when the addition of $100 \text{ mg} \cdot \text{L}^{-1}$ of BPA) were found to be less than 1.0, suggesting that the simultaneous presence of both phenolic compound molecules reduced the adsorption through competition for binding sites on the OAB [4]. Moreover, the TCP q_e^b/q_e^s value is greater than that of BPA and shows that in the presence of competition of phenolic compounds, adsorption effect of BPA on OAB is larger than it is for TCP. The results confirmed that the preferential adsorption by OAB was given to the TCP. This difference in behavior is attributed to the different octanol-water partitioning coefficients ($\log K_{ow}$) of each compound, which results in different hydrophobic interaction densities with organoclay. TCP is more hydrophobic, and its $\log K_{ow}$ value (3.66) is higher than of BPA (3.32). The difference between the hydrophobic and hydrophilic regions of BPA and TCP determine the extent of the sorption affinity, resulting in the preferential sorption of OAB for TCP. Similar phenomena have been observed by Jianming et al. [45].

3.10. Desorption of BPA/TCP and reuse of OAB

Four regeneration adsorption capacities of OAB are shown in Fig. 9 for two phenolic compounds. It was observed that at the first adsorption step, the adsorption capacities for the TCP and BPA reached the values of 92 and $89 \text{ mg} \cdot \text{g}^{-1}$, respectively. As seen from the figure, the total adsorption capacities of both TCP and BPA slightly decreased after four-time regeneration; not more than 13 and 20% when compared with the virgin adsorption capacity for TCP and BPA, respectively. This could be ascribed to the fact that the regeneration process might result in the decrease of binding sites [4,44]. In addition, the percentages desorption of BPA and TCP was decreased from 90 to 75% and from 87 to 70%, respectively. Therefore, this study indicates that the OAB is a suitable and excellent material for multiple uses in the removal of BPA and TCP from aqueous solutions.

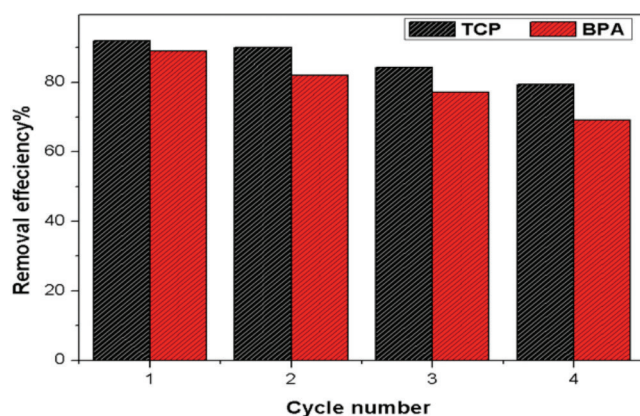


Fig. 9. Adsorption/desorption cycles of TCP and BPA onto OAB.

4. Conclusions

In the present investigation, the modified Algerian bentonite (OAB) was successfully prepared and evaluated as an adsorbent for the adsorption of BPA and TCP in single and binary solution systems. The synthesized organo-acid-activated bentonite was characterized using various techniques. It is found that when the surfactant loading increases, structural changes of CTAB molecules occur, leading to expanded basal spacings. The characterized OAB was tested for their abilities to remove BPA and TCP from aqueous solutions and the experiments showed that the OAB is more effective in removing TCP than BPA. The experimental data of adsorption kinetics are well described by pseudo-second-order kinetic equation. The equilibrium isotherm of phenolic compounds is found to be well represented by the Langmuir and Freundlich models for removal of BPA/TCP, respectively. In binary system, BPA adsorption onto OAB was more affected by the simultaneous presence of TCP, and OAB has an excellent regeneration property.

Acknowledgments

Nassima Djebri (doctorante) acknowledges the Laboratory of chemical engineering (LGPC) of the university of Setif, Algeria for the financial support of this work. Special gratitude to Prof. Djellouli Brahim and Prof. Saci Nacef for their technical support.

References

- [1] H. Wu, G. Li, S. Liu, N. Hu, D. Geng, G. Chen, Z. Sun, X. Zhao, L. Xia, J. You, Monitoring the contents of six steroidal and phenolic endocrinedisrupting chemicals in chicken, fish and aquaculture pond water samples using pre-column derivatization and dispersive liquid-liquid microextraction with the aid of experimental design methodology. *Food. Chem.*, 192 (2016) 98–106.
- [2] Z.L. Zhang, A. Hibberd, J.L. Zhou, Optimisation of derivatisation for the analysis of estrogenic compounds in water by solid-phase extraction gas chromatography-mass spectrometry. *Anal. Chim. Acta.*, 577 (2006) 52–61.
- [3] B.R. Lim, S.H. Do, S.H. Hong, The impact of humic acid on the removal of Bisphenol A by adsorption and Ozonation. *Desal. Water Treat.*, 54 (2015) 1226–1232.
- [4] X. Zheng, J. Dai, J. Pan, Synthesis of β -cyclodextrin/mesoporous attapulgite composites and their novel application in adsorption of 2,4,6-trichlorophenol and 2,4,5-trichlorophenol. *Desal. Water Treat.*, 57 (2016) 14241–14250.
- [5] E.B. Simsek, B. Aytas, D. Duranoglu, U. Beker, W. Andrzej Trochimczuk, A comparative study of 2-chlorophenol, 2,4-dichlorophenol, and 2,4,6-trichlorophenol adsorption onto polymeric, commercial, and carbonaceous adsorbents. *Desal. Water Treat.*, 57 (2016) 9940–9956.
- [6] J.M. Ahmed, K.S. Theydan, Equilibrium isotherms, kinetics and thermodynamics studies of phenolic compound adsorption on palm-tree fruit stones, *Ecotox. Environ. Safety*, 84 (2012) 39–45.
- [7] H. Wang, H. Zhang, J.Q. Jiang, X. Ma, Adsorption of bisphenol A onto cationic-modified zeolite. *Desal. Water Treat.*, 57(54) (2016) 26299–26306.
- [8] J. Hoigne, Organic micro pollutants and treatment processes: kinetics and final effect ozone and chloride dioxide. *Sci. Total Environ.*, 47 (1985) 169–185.
- [9] L. Ukrainczyk, M.B. McBride, Oxidation of phenol in acidic aqueous suspensions of manganese oxides. *Clays Clay Miner.*, 40 (1992) 157–166.

- [10] J. Kochany, J.R. Bolton, Mechanism of photo degradation of aqueous organic pollutants. *Environ. Sci. Technol.*, 31 (1992) 50–53.
- [11] L. Zhang, B. Zhang, T. Wu, D. Sun, Y. Li, Adsorption behavior and mechanism of chlorophenols onto organoclays in aqueous solution. *Colloids. Surf. A. Physicochem. Eng. Asp.*, 484 (2015) 118–129.
- [12] Z.N. Garba, A.A. Rahim, Optimization of activated carbon preparation conditions from *Prosopis Africana* seed hulls for the removal of 2,4,6-trichlorophenol from aqueous solution. *Desal. Water Treat.*, 56 (2015) 2879–2889.
- [13] S.B. McGray, R.J. Ray, Concentration of sinful processes condensate by reverse osmosis. *Separ. Sci. Tech.*, 22 (1987) 745.
- [14] L. Joseph, J. Heo, Y.G. Park, J.R.V. Flora, Y. Yoon, Adsorption of bisphenol A and 17 α -ethinylestradiol on single walled carbon nanotubes from seawater and brackish water. *Desalination*, 281 (2011) 68.
- [15] Y.H. Kim, B. Lee, K.H. Choo, S.J. Choi, Adsorption characteristics of phenolic and amino organic compounds on nano-structured silicas functionalized with phenyl groups. *Micropor. Mesopor. Mater.*, 185 (2014) 121–129.
- [16] H.Z. Boudiaf, M. Boutahala, Adsorption of 2,4,5-trichlorophenol by organo-montmorillonites from aqueous solutions: Kinetics and equilibrium studies. *Chem. Eng. J.*, 170 (2011) 120–126.
- [17] K. Naddafi, N. Rastkari, R. Nabizadeh, R. Saeedi, M. Gholami, M. Sarkhosh, Adsorption of 2,4,6-trichlorophenol from aqueous solutions by a surfactant-modified zeolitic tuff: batch and continuous studies. *Desal. Water Treat.*, 57 (2016) 5789–5799.
- [18] M.R. Hartono, R.S. Marks, X. Chen, A. Kushmaro, Hybrid multi-walled carbon nanotubes-alginate-polysulfone beads for adsorption of bisphenol-A from aqueous solution. *Desal. Water Treat.*, 54 (2015) 1167–1183.
- [19] Z. Zhao, D. Fu, B. Zhang, Novel molecularly imprinted polymer prepared by palygorskite as support for selective adsorption of bisphenol A in aqueous solution. *Desal. Water Treat.*, 57 (2016) 12433–12442.
- [20] H.Z. Boudiaf, M. Boutahala, Equilibrium and kinetics studies of 2,4,5-trichlorophenol adsorption onto organophilic-bentonite. *Desal. Water Treat.*, 24 (2010) 47–54.
- [21] Y. Park, Z. Sun, G.A. Ayoko, R.L. Frost, Bisphenol A sorption by organo-montmorillonite: Implications for the removal of organic contaminants from water. *Chemosphere*, 107 (2014) 249–256.
- [22] P. Komadel, Acid activated clays: Materials in continuous demand. *Appl. Clay Sci.* (2016) DOI: 10.1016/j.clay.2016.05.001
- [23] H.Z. Boudiaf, M. Boutahala, Preparation and characterization of organo-montmorillonites. Application in adsorption of the 2,4,5-trichlorophenol from aqueous solution, *Adv. Powder Technol.*, 22 (2011) 735–740.
- [24] M.R. Hartono, R.S. Marks, X. Chen, A. Kushmaro, Hybrid multi-walled carbon nanotubes-alginate-polysulfone beads for adsorption of bisphenol-A from aqueous solution. *Desal. Water Treat.*, 54 (2015) 1167–1183.
- [25] Q. Yang, M. Gao, Z. Luo, S. Yang, Enhanced removal of bisphenol A from aqueous solution by organomontmorillonites modified with novel Gemini pyridinium surfactants containing long alkyl chain. *Chem. Eng. J.*, 285 (2016) 27–38.
- [26] F. Gomri, M. Boutahala, H.Z. Boudiaf, S.A. Korili, A. Gil, Removal of acid blue 80 from aqueous solutions by adsorption on chemical modified bentonites. *Desal. Water Treat.*, 57(54) (2016) 26240–26249.
- [27] C.H. Giles, T.H. McEwan, S.N. Nakhwa, D. Smith, Studies in adsorption. Part XI. A system of classification of solution adsorption isotherms, and its use in diagnosis of adsorption mechanisms and in measurement of specific surface areas of solids. *J. Chem. Soc.*, 111 (1960) 3973–3993.
- [28] H. Noyan, M. Önal, Y. Sarıkaya, The effect of sulfuric acid activation on the crystallinity, surface area, porosity, surface acidity, and bleaching power of a bentonite. *Food. Chem.*, 105 (2007) 156–163.
- [29] H.Z. Boudiaf, M. Bouhatala, S. Sahnoun, C. Tiar, F. Gomri, Adsorption characteristics, isotherm, kinetics, and diffusion of modified natural bentonite for removing the 2,4,5-trichlorophenol. *Appl. Clay Sci.*, 90 (2014) 81–87.
- [30] Y. Seki, K. Yurdakoç, Paraquat adsorption onto clays and organo-clays from aqueous solution. *J. Colloid Interface Sci.*, 287 (2005) 1–5.
- [31] C. Namasivayam, D. Kavitha, Removal of phenol and chlorophenols from water by coir pith carbon. *J. Environ. Sci. Eng.*, 46 (2003) 217–232.
- [32] M. Radhika, K. Palanivelu, Adsorptive removal of chlorophenols from aqueous solution by low cost adsorbent: kinetics and isotherm analysis. *J. Hazard. Mater.*, B138 (2006) 116–124.
- [33] B.H. Hameed, Equilibrium and kinetics studies of 2,4,6-trichlorophenol adsorption onto activated clay. *Colloids. Surf. A. Physicochem. Eng. Asp.*, 307 (2007) 45–52.
- [34] B.H. Hameed, I.A.W. Tan, A.L. Ahmad, Adsorption isotherm, kinetic modeling and mechanism of 2,4,6-trichlorophenol on coconut husk-based activated carbon. *Chem. Eng. J.*, 144 (2008) 235–244.
- [35] R. Rawajfih, N. Nsour, Characterizations of phenols and chlorinated phenols sorption onto surfactant-modified bentonite. *J. Colloid Interface Sci.*, 298 (2006) 39–49.
- [36] G. Xue, M. Gao, Z. Gu, Z. Luo, Z. Hu, The removal of p-nitrophenol from aqueous solutions by adsorption using Gemini surfactants modified montmorillonites. *Chem. Eng. J.*, 218 (2013) 223–231.
- [37] S. Sahnoun, M. Boutahala, H.Z. Boudiaf, L. Zerroual, Trichlorophenol removal from aqueous solutions by modified halloysite: kinetic and equilibrium studies. *Desal. Water Treat.*, 57 (2016) 15941–15951.
- [38] C. Moreno-Castilla, J. Rivera-Utrilla, M.V. López-Ramón, F. Carrasco-Marín, Adsorption of some substituted phenols on activated carbons from bituminous coal. *Carbon*, 33 (1995) 845.
- [39] Y. Angar, N.-E. Djelali, S. Kebbouche-Gana, Kinetic and thermodynamic studies of the ammonium ions adsorption onto natural Algerian Bentonite. *Desal. Water. Treat.*, 57(53) (2016) 25696–25704.
- [40] Q. Sui, J. Huang, Y. Liu, X. Chang, G. Ji, S. Deng, T. Xie, G. Yu, Rapid removal of bisphenol A on highly ordered mesoporous carbon. *J. Environ. Sci.*, 23 (2011) 177–182.
- [41] H.Z. Boudiaf, M. Boutahala, C. Tiar, L. Arab, F. Garin, Treatment of 2,4,5-trichlorophenol by MgAl-SDBS organo-layered double hydroxides: Kinetic and equilibrium studies. *Chem. Eng. J.*, 173 (2011) 36–41.
- [42] J. Wang, J. Pan, Y. Yin, R. Wu, X. Dai, J. Dai, L. Gao, H. Ou, Thermo-responsive and magnetic molecularly imprinted Fe₃O₄@carbon nano-spheres for selective adsorption and controlled release of 2,4,5-trichlorophenol. *J. Ind. Eng. Chem.*, 25 (2015) 321–328.
- [44] Y. Zhou, P. Lu, J. Lu. Application of nature biosorbent and modified peat for bisphenol A removal from aqueous solutions. *Carbohydr. Polym.*, 88 (2012) 502–508.
- [45] J. Pan, H. Yao, X.X. Li, B. Wang, P. Huo, W. Xu, H. Ou, Y. Yan, Synthesis of chitosan/Fe₂O₃/fly-ash-cenospheres composites for the fast removal of bisphenol A and 2,4,6-trichlorophenol from aqueous solutions. *J. Hazard. Mater.*, 190 (2011) 276–284.